

Received August 10, 2014, accepted September 13, 2014, date of publication September 17, 2014, date of current version September 26, 2014.

Digital Object Identifier 10.1109/ACCESS.2014.2358954

# Adaptive Sliding Mode Observer for Engine Cylinder Pressure Imbalance Under Different Parameter Uncertainties

AHMED AL-DURRA, (Senior Member, IEEE)

Department of Electrical Engineering, Petroleum Institute, Abu Dhabi 2533, United Arab Emirates

Corresponding author: A. Al-Durra (aaldurra@pi.ac.ae)

This work was supported by the Center for Automotive Research, Ohio State University, Columbus, OH, USA.

**ABSTRACT** One of the principal issues of alternative combustion modes for diesel engines (such as HCCI, PCCI, and LTC) is caused by the imbalances in the distribution of air and EGR across the cylinders, which affects the combustion process and ultimately cause significant differences in the pressure trace and indicated torque for each cylinder. In principle, a cylinder-by-cylinder control approach could compensate for air, residuals, and temperature imbalance. However, in order to fully benefit from closed-loop combustion control, it is necessary to obtain feedback signals from each engine cylinder to reconstruct the pressure trace. Therefore, cylinder imbalance is an issue that can be detected in a laboratory environment, wherein each engine cylinder is instrumented with a dedicated pressure transducer. This paper describes the framework and preliminary results of a model-based estimation approach to predict the individual pressure traces in a multicylinder engine relying on a very restricted sensor set, namely, a crankshaft speed sensor, a single production-grade pressure sensor. The objective of the estimator is to reconstruct the complete pressure trace during an engine cycle with sufficient accuracy to allow for detection of cylinder to cylinder imbalances. Starting from a model of the engine crankshaft dynamics, an adaptive sliding mode observer is designed to estimate the cylinder pressure from the crankshaft speed fluctuation measurement. The results obtained by the estimator are compared with experimental data obtained on a four-cylinder diesel engine.

**INDEX TERMS** Engine, cylinder pressure imbalance, sliding mode observer, adaptive observer, parameter uncertainty.

## I. INTRODUCTION

Conventional Diesel engines typically operate in open loop with respect to combustion [1]. As emissions and diagnostic regulations have become more stringent, the possibility of closed-loop combustion control has recently gained interest [2]. In particular, the possibility of controlling the individual fuel injectors could help compensating for several sources of variability, such as the air and residual mass imbalance that occurs between cylinders and leads to differences in cylinder pressure traces, engine torque and emissions [3].

In principle, a cylinder-by-cylinder control approach could compensate for air, residuals and temperature imbalance [3]. However, in order to fully benefit of closed-loop combustion control, it is necessary to obtain feedback from each engine cylinder to reconstruct the pressure trace. Processing cylinder pressure data for real-time applications requires several operations to be performed in order to eliminate the noise and offset issues associated to the output of piezoelectric transducers [4]. However, the signal processing operations that are performed on the sensors outputs lead to delays

in the estimation of the pressure, therefore preventing from real-time applications.

Furthermore, due to cost issues, the use of a dedicated piezoelectric transducer per engine cylinder is today limited to laboratory testing. For light-duty automotive applications, the use of sensors in every cylinder will likely be cost prohibitive, and it is likely that only one sensor per cylinder bank will be utilized in the next generation of control systems. This will require more sophisticated estimation techniques to detect the pressure in the remaining engine cylinders, for instance by processing the engine crankshaft speed fluctuations [5]–[10]. Torque estimation from crankshaft speed sensing has been largely utilized in the past for combustion diagnostics, for example misfire detection [11]–[13]. However, it appears evident that such estimation methods are not accurate enough to diagnose torque imbalances due to the air and EGR distribution through the cylinders.

In summary, in order to take advantage of Diesel engine closed loop combustion control to compensate for cylinder imbalance, it is necessary to develop an estimation

methodology that allows for an accurate prediction of the pressure trace in each individual cylinder with real-time capabilities and minimal sensor requirements.

The scope of this work is to demonstrate a model-based estimation methodology that allows one for the real-time reconstruction of individual in-cylinder pressures, utilizing a minimum sensor set. The outcome of this work will be an algorithm that could be implemented into a closed-loop control system for automotive Diesel engines utilizing cylinder pressure feedback to compensate for imbalances due to air and EGR distribution.

## II. CRANKSHAFT MODEL STRUCTURE

Following the approach proposed in [14], a dynamic model of the in-cylinder processes based on the energy conservation principle is here applied to predict the cylinder pressure from intake valve closing to exhaust valve opening (IVC→EVO). This model is here extended to an inline four-cylinder engine by properly phasing the combustion events based on the firing order of the engine and by approximating the pressure during the charge exchange phase of the cycle to a constant term. As a result, the pressures  $p_{cyl,1}, \dots, p_{cyl,4}$  of the four cylinders are defined by the following equation:

$$\begin{cases} \frac{dp_{cyl,i}}{d\theta_i} + \frac{\gamma}{V_{cyl}} \frac{dV_{cyl}}{d\theta_i} p_{cyl,i} \\ = \frac{\gamma-1}{V_{cyl}} \left[ (1-\alpha) \frac{dQ_g}{d\theta_i} \right] & \text{if } \theta_{IVC} \leq \theta_i \leq \theta_{EVO} \\ p_{cyl,i} = p_{IM} & \text{otherwise} \end{cases} \quad (1)$$

for  $i = 1, \dots, 4$ , where the crank angle is defined as:

$\theta_1 = \text{rem}(\theta, 4\pi)$	Cylinder 1
$\theta_2 = \text{rem}(\theta + \pi, 4\pi)$	Cylinder 2
$\theta_3 = \text{rem}(\theta + 3\pi, 4\pi)$	Cylinder 3
$\theta_4 = \text{rem}(\theta + 2\pi, 4\pi)$	Cylinder 4

The apparent gross heat release rate  $Q_g$  in Equation (1) accounts for the fuel energy released during the combustion and the heat losses due to heat transfer to the cylinder walls [15]. This term is estimated through the definition of an apparent fuel burning rate, which is modeled as a linear combinations of Wiebe functions calibrated on steady-state experimental data [16].

The cylinder pressure is used to calculate the instantaneous indicated torque  $T_{ind,i}(\theta_i)$ , acting on the crank arm [14], [17], [18]. In addition to the indicated torque, the reciprocating inertia torque  $T_{m,i}(\theta_i, \omega)$  and the engine friction torque  $T_{fr}(\omega)$  must be modeled in order to determine the effective torque acting on the crank arm [15]. The above terms have been calculated as in [18].

Finally, a simple, one-degree of freedom model of the the rotational dynamics of the crankshaft system is defined by a

torque balance, assuming the crankshaft as a rigid body:

$$\frac{d\omega(\theta)}{d\theta} = \sum_{i=1}^4 \left( \frac{T_{ind,i}(\theta_i) + T_{m,i}(\theta_i, \omega)}{J_{eq}\omega} \right) - \frac{T_{fr}(\omega) + T_{load}}{J_{eq}\omega} \quad (2)$$

where  $J_{eq}$  is the equivalent inertia of the engine cranktrain.

In order to facilitate the design of the estimator, a simplification is introduced in the model. Specifically, it is assumed from here on that each torque pulse produced by a firing event causes a distinct fluctuations in crankshaft velocity and acceleration [5], [9], [19]. This allows one to decouple each cylinder pressure event which generates a torque contribution in Equation 2.

The complete engine cylinder pressure and crankshaft dynamics model given by Equations (1)-(2) can be converted to state-space form to facilitate the estimator design. To this end, the model is slightly approximated by assuming the reciprocating inertia torque as acting with the engine load as an external torque, and its value calculated from the estimated engine speed. Such approximation is accepted for a light-duty Diesel engine, where the indicated torque is an order of magnitude higher than the reciprocating inertia torque [18]. Furthermore, let:

- $A_{11}(\omega) = \frac{-k_{\omega_1} - k_{\omega_2}\omega}{J_{eq}\omega}$
- $A_{12}(\theta_i, \omega) = \frac{rA_{pf}(\theta_i)}{J_{eq}\omega}$
- $A_{22}(\theta_i, \omega) = -\frac{\gamma}{V_{cyl}(\theta_i)} \frac{dV_{cyl}(\theta_i)}{d\theta_i}$
- $N(\theta_i) = \frac{\gamma-1}{V_{cyl}(\theta_i)} \frac{dQ_n(\theta_i)}{d\theta}$
- $H(\theta, \omega) = \sum_{i=1}^4 \frac{T_{m,i} - rA_{pambf}(\theta_i) - T_{fr0} - T_{load}}{J_{eq}\omega}$

These assumptions and notations lead to the following state representation form:

$$\begin{bmatrix} \frac{d\omega}{d\theta} \\ \frac{dp_{cyl}}{d\theta} \end{bmatrix} = \begin{bmatrix} A_{11}(\omega) & A_{12}(\theta, \omega) \\ 0 & A_{22}(\theta, \omega) \end{bmatrix} \begin{bmatrix} \omega \\ p_{cyl} \end{bmatrix} + \begin{bmatrix} H(\theta, \omega) \\ N(\theta) \end{bmatrix} \quad (3)$$

where  $p_{cyl} = [p_{cyl,1}, \dots, p_{cyl,4}]^T$  and

- $A_{12}(\theta, \omega) = [A_{12}(\theta_1, \omega), \dots, A_{12}(\theta_4, \omega)]$
- $A_{22}(\theta, \omega) = \text{diag}\{A_{22}(\theta_1, \omega), \dots, A_{22}(\theta_4, \omega)\}$
- $N(\theta) = \text{diag}\{N(\theta_1), \dots, N(\theta_4)\}$

Finally, let  $x = [\omega \ p_{cyl}^T]^T$  and

$$y = Cx = \begin{bmatrix} 1 & 0 \end{bmatrix} x = x_1 = \omega \quad (4)$$

In the above form, the model can be tested for observability, which is a necessary condition for the estimator design. To study the uniform observability of the system, the matrix

$$\Lambda(\theta) = \begin{bmatrix} C \\ \dot{C} + CA \end{bmatrix} = \begin{bmatrix} 1 & 0 \\ A_{11} & A_{12} \end{bmatrix} \quad (5)$$

must be of full rank for each angular position. The system described by Equation 3 results uniformly observable except at top dead center (TDC) and bottom dead center (BDC), where the condition  $A_{12} = 0$  occurs [14]. This is physically reasonable, as the cylinder pressure has no effects on the crankshaft speed when the piston is located at its extreme positions.

### III. ESTIMATION SCHEME

A simple schematic of an inline four-cylinder engine is shown in Figure 1. The proposed estimation scheme relies on the output of a single production-grade pressure transducer (for example, located in cylinder 1), and on the engine crankshaft speed sensor output to predict the pressure trace for each individual cylinder.

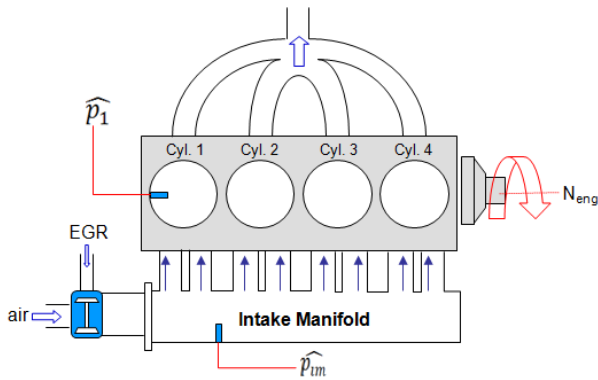


**FIGURE 1.** Schematic of four-cylinder engine showing the sensor configuration utilized in the proposed estimation scheme.

Preliminary work has been done on the analysis of the raw signal from the piezoelectric sensors and on the real-time estimation of cylinder pressure [20]. The outcome is a model-based estimation algorithm that consists of an Extended Kalman Filter (EKF) augmented with recursive least square (RLS) estimator. The estimator relies on a control-oriented thermodynamic model of the in-cylinder process to characterize the cylinder pressure trace in real-time conditions (on a crank-angle basis), given the engine operating condition in term of mean engine speed and load (represented by the total injected fuel quantity). The estimator has been validated on experimental data from a laboratory test bench [14], [21].

The work in [21] focused on the feasibility of extending the estimation algorithm developed in [14] to a multi-cylinder Diesel engine, to predict the cylinder pressures utilizing a minimal sensor set. The proposed estimation scheme is shown in Figure 2. The model-based estimator utilized the inputs from a single pressure transducer (for example, located in cylinder 1 as in figure 1) and from the engine crankshaft speed sensor to reconstruct the individual pressure of each cylinder for a representative engine condition.

The cylinder pressure was estimated using sliding mode observer based on the crankshaft speed measurement only. The work done in [21] can be improved by implementing

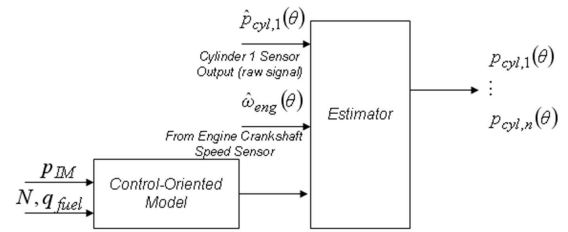


**FIGURE 2.** Conceptual block diagram for the proposed multi-cylinder pressure estimation with limited sensing.

the SMO in an adaptive way rather than assuming full and accurate information in the model which is the major contribution of this paper.

### IV. ADAPTATION USING ONE CYLINDER PRESSURE MEASUREMENT

To accommodate for the uncertainties, the model form is slightly modified to be

$$\begin{bmatrix} \frac{dx_1}{d\theta} \\ \frac{dx_2}{d\theta} \end{bmatrix} = \begin{bmatrix} A_{11}(\theta) & A_{12}(\theta) \\ 0 & A_{22}(\theta) \end{bmatrix} \begin{bmatrix} x_1 \\ x_2 \end{bmatrix} + \begin{bmatrix} H(\theta) & 0 \\ 0 & N(\theta) \end{bmatrix} \begin{bmatrix} \mu_1 \\ \mu_2 \end{bmatrix} \quad (6)$$

where  $A_{11}$ ,  $A_{12}$ , and  $A_{22}$  are defined as in Equation 3.  $\mu_1$  is the uncertainty variable for the engine friction offset and  $\mu_2$  is the uncertainty variable which can be interpreted as a scaling factor of the gross heat release. The assumption made here is that the friction offset and the heat transfer are the same for all cylinders.

Using the Certainty Equivalence Principle, the sliding mode observer can be designed assuming  $\mu_1$  and  $\mu_2$  are known, as was done in Section III. To deal with the uncertainties, an adaptive-SMO can be derived by introducing the uncertainty to the error dynamics as follows:

$$\frac{d\tilde{y}}{d\theta} = A_{11}\tilde{y} + A_{12}\tilde{x}_2 + \tilde{\mu}_1 H(\theta) - K \text{sign}(\tilde{y}), \quad (7a)$$

$$\frac{d\tilde{x}_2}{d\theta} = A_{22}\tilde{x}_2 + \tilde{\mu}_2 N(\theta) - LK \text{sign}(\tilde{y}). \quad (7b)$$

After the enforcement of the sliding mode ( $\tilde{y} \rightarrow 0$ ) as explained earlier, the equivalent control becomes:

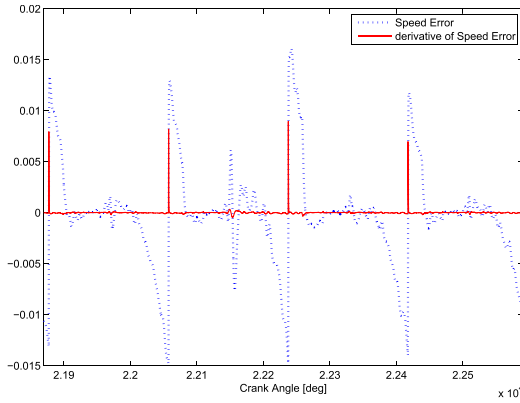
$$V_{eq} = A_{12}\tilde{x}_2 + \tilde{\mu}_1 H(\theta), \quad (8)$$

and the motion equation is

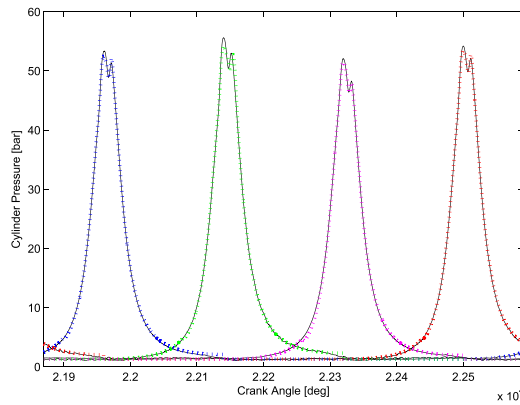
$$\begin{aligned} \frac{d\tilde{x}_2}{d\theta} &= A_{22}\tilde{x}_2 + \tilde{\mu}_2 N(\theta) - LA_{12}\tilde{x}_2 + L\tilde{\mu}_1 H(\theta) \\ &= (A_{22} - LA_{12})\tilde{x}_2 + \tilde{\mu}_2 N(\theta) + L\tilde{\mu}_1 H(\theta), \end{aligned} \quad (9)$$

where  $L(\theta)$  is designed to make the term  $(A_{22} - LA_{12})$  negative as in the case with no uncertainty. The goal now is to find  $\frac{d\tilde{\mu}_1}{d\theta}$  and  $\frac{d\tilde{\mu}_2}{d\theta}$  such that the overall error system  $(\tilde{x}_2, \tilde{\mu}_1, \tilde{\mu}_2)$  converges to the origin. A Lyapunov candidate function can be used here as follows ( $\nu_1, \nu_2 > 0$  are the adaptation gains):

$$V = \frac{1}{2}\tilde{x}_2^2 + \frac{1}{2\nu_1}\tilde{\mu}_1^2 + \frac{1}{2\nu_2}\tilde{\mu}_2^2 \quad (10)$$



(a)



(b)

**FIGURE 3.** Results using experimental pressure traces with disturbances applied to adaptive observer. Left to right, the peaks represent cylinders 1, 3, 4, and 2. (a) Crankshaft speed estimation error (dotted) and crankshaft acceleration error (solid) for test-1 case. (b) Cylinder Pressures data (solid) and Estimated (dotted) for test-1 case (experimental).

and

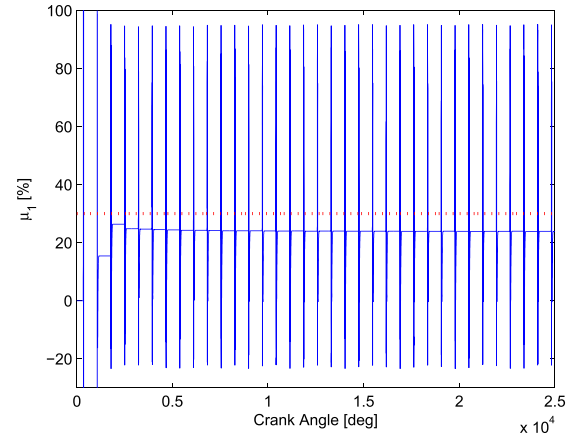
$$\begin{aligned} \frac{dV}{d\theta} &= \tilde{x}_2[(A_{22} - LA_{12})\tilde{x}_2 + \tilde{\mu}_2 N(\theta) - L\tilde{\mu}_1 H(\theta)] \\ &\quad - \frac{1}{v_1} \tilde{\mu}_1 \frac{d\hat{\mu}_1}{d\theta} - \frac{1}{v_2} \tilde{\mu}_2 \frac{d\hat{\mu}_2}{d\theta} \\ &= (A_{22} - LA_{12})(\tilde{x}_2)^2 + \tilde{\mu}_2(\tilde{x}_2 N(\theta) - \frac{1}{v_2} \frac{d\hat{\mu}_2}{d\theta}) \\ &\quad + \tilde{\mu}_1(-\tilde{x}_2 LH(\theta) - \frac{1}{v_1} \frac{d\hat{\mu}_1}{d\theta}). \end{aligned} \quad (11)$$

By designing the adaptive parameters dynamics as

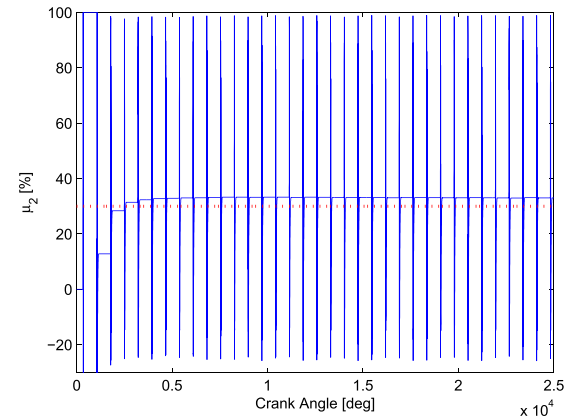
$$\frac{d\hat{\mu}_1}{d\theta} = -v_1 \tilde{x}_2 LH(\theta), \quad (12a)$$

$$\frac{d\hat{\mu}_2}{d\theta} = v_2 \tilde{x}_2 N(\theta), \quad (12b)$$

we can enforce  $\frac{dV}{d\theta} \leq 0$ , implying stability of the error system based on Lyapunov stability theory. There are two points to be discussed based on this result. First, the adaptation dynamics require a value for the pressure error, which in



(a)



(b)

**FIGURE 4.** Estimated deviation in the uncertainty parameters  $\mu_1$  and  $\mu_2$ .

turn requires feedback from the cylinder pressure; this, then, justifies the need for this sensor in one cylinder. Second, for the error system to converge to the origin, the system must be asymptotically stable (not simply stable).

To assure asymptotic stability, the La Salle/Yoshizawa Theorem will be utilized. It can be proven that the estimator error  $\tilde{x}_2$  will converge to the origin (see Appendix for details on the theorem):

- 1) Let  $W(\tilde{x}_2) = \lambda_{\max}(A_{22} - LA_{12})(\tilde{x}_2)^2$ , which is negative definite ( $W(\tilde{x}_2) < 0$ ) by design  $\forall \theta$  except at TDC, as discussed in [21].
- 2) Therefore,  $\frac{dV}{d\theta} \leq W(\tilde{x}_2)$ , which satisfies the hypothesis of the theorem.
- 3) As a consequence of the theorem,  $W(\tilde{x}_2) \rightarrow 0$ .
- 4) This implies that  $\tilde{x}_2 \rightarrow 0$  except at the instant of TDC.

This result proves provides an analytical proof for the asymptotic stability of the pressure estimation error, which is our ultimate goal. One drawback from this result is the lack of a notion of *uniform* convergence. Uniform convergence leads to *total stability*, i.e. stability under persistent disturbance [22]. This does not necessarily mean that the estimator with this derivation is not robust, but it puts more concerns on

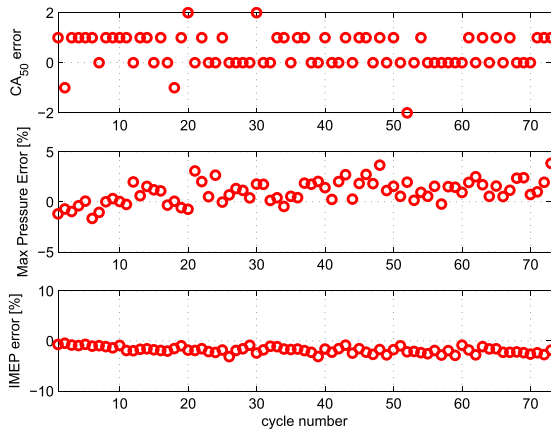


**FIGURE 5.** Errors in the estimation of the cycle-by-cycle combustion metrics with disturbances and adaptation (cylinder-1 and test-1).

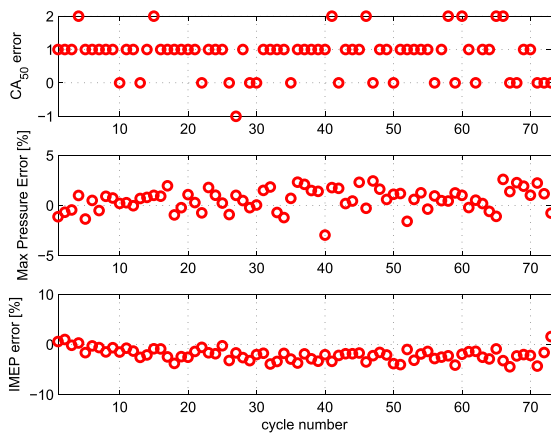


**FIGURE 6.** Errors in the estimation of the cycle-by-cycle combustion metrics with disturbances and adaptation (cylinder-2 and test-1).

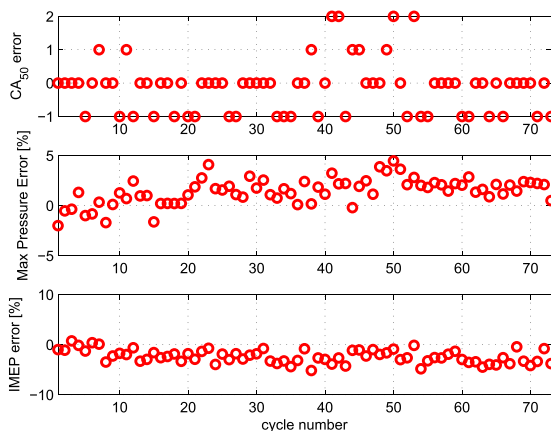


**FIGURE 7.** Errors in the estimation of the cycle-by-cycle combustion metrics with disturbances and adaptation (cylinder-3 and test-1).

the level of disturbances and signal noise that the estimator can handle.

Figure 3 shows the results using the adaptive-SMO with the same model and disturbances applied in the previous section. The results show a better performance (compared to

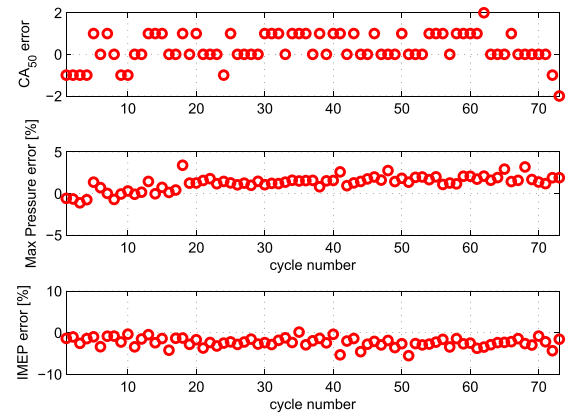
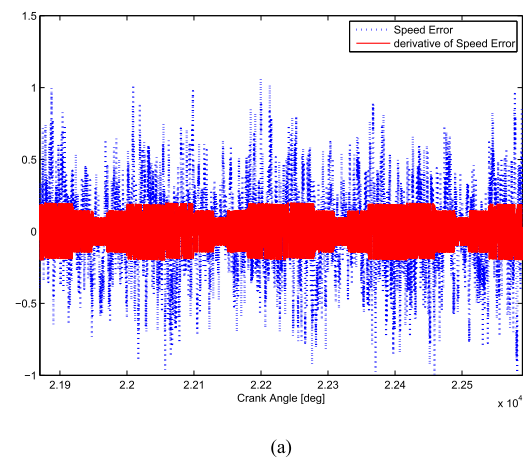
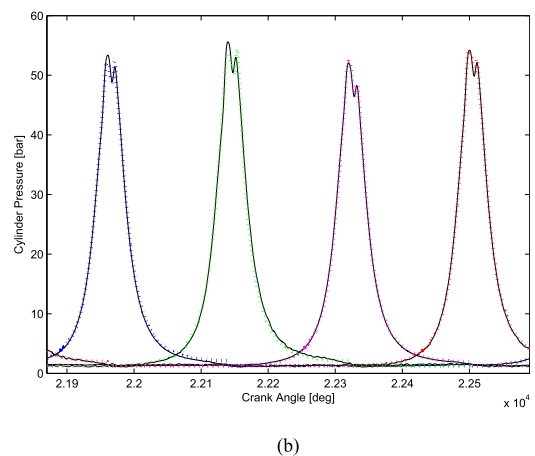


**FIGURE 8.** Errors in the estimation of the cycle-by-cycle combustion metrics with disturbances and adaptation (cylinder-4 and test-1).



(a)



(b)

**FIGURE 9.** Results using experimental pressure traces with disturbances and noisy crankshaft speed signal applied to adaptive observer. Left to right, the peaks represent cylinders 1, 3, 4, and 2. (a) Crankshaft speed estimation error (dotted) and crankshaft acceleration error (solid) for test-1 case. (b) Cylinder Pressures data (solid) and Estimated (dotted) for test-1 case (experimental).

SMO-Only observer in [21]) in terms of less speed error as well as better tracking for the pressure traces (note that the second peak is perfectly captured). As mentioned earlier,



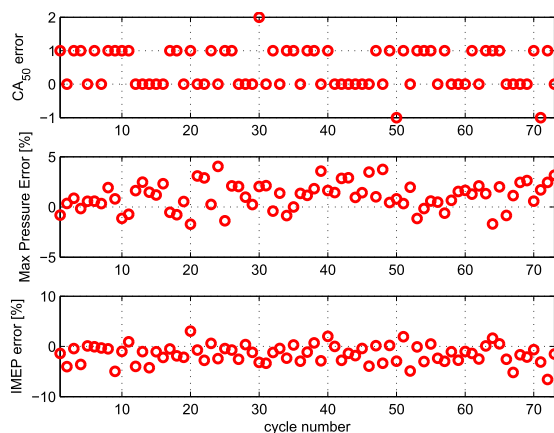


**FIGURE 10.** Errors in the estimation of the cycle-by-cycle combustion metrics with disturbances, noise and adaptation (cylinder-1 and test-1).

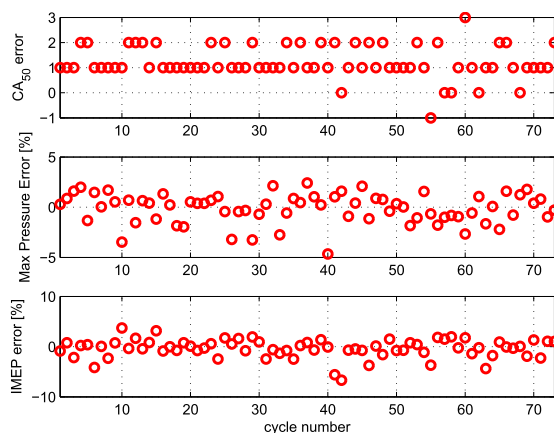


**FIGURE 11.** Errors in the estimation of the cycle-by-cycle combustion metrics with disturbances, noise and adaptation (cylinder-2 and test-1).

the estimator design which is based on La Salle/Yoshizawa Theorem lacks the Uniform Convergence; consequently, the estimation of the deviation in the uncertainty parameters,  $\mu_1$  and  $\mu_2$ , is not converging to the 30% which was the preset value as shown in Figure 4; however, the estimation is still stable. The short duration fluctuations in the estimation are results of the lack of observability at the instant of TDC.

In terms of the combustion metrics, Figure 5 shows a great improvement, especially in terms of  $CA_{50}$  and  $IMEP$  compared to the case without adaptation. Figures 6, 7, and 8 show the combustion metrics for the other cylinders (2, 3, and 4), where the estimation is still better than the case without adaptation. However, these estimation results are not as good as the result for cylinder-1 because the cylinder pressure signal was generated from cylinder-1.

The estimator can be further tested by adding white Gaussian noise of 10 RPM standard deviation to the crankshaft speed feedback signal. The result shown in Figure 9 looks very promising since the estimator is able to reconstruct the pressure with a very good accuracy despite the noisy speed measurement.

Finally, the estimation for the combustion metrics for the four cylinder are shown in Figures 10, 11, 12, and 13.

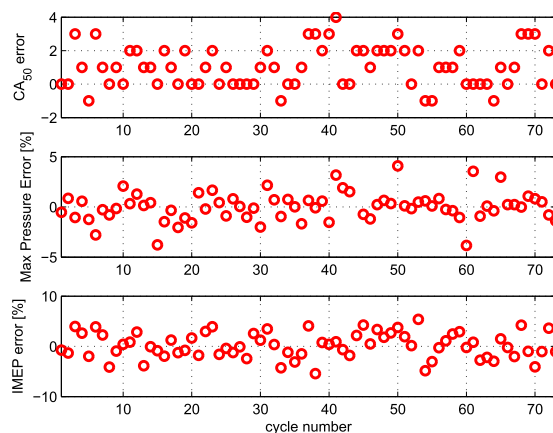


**FIGURE 12.** Errors in the estimation of the cycle-by-cycle combustion metrics with disturbances, noise and adaptation (cylinder-3 and test-1).

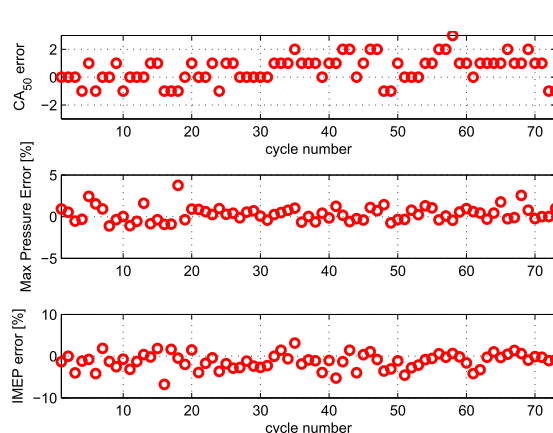


**FIGURE 13.** Errors in the estimation of the cycle-by-cycle combustion metrics with disturbances, noise and adaptation (cylinder-4 and test-1).

We notice more fluctuation because of the noise, but the result overall seems very acceptable.

## V. CONCLUSION

The scope of this work has been to demonstrate a model-based estimation methodology that facilitates real-time reconstruction of individual in-cylinder pressure, utilizing a minimum sensor set. The first step was to derive a crankshaft speed model incorporated with the pressure model derived in [20]. The sliding mode observer implemented in [21] was improved by the development of an adaptive-SMO based on the certainty equivalence principle and utilizing the cylinder pressure signal from one cylinder. The estimator was derived analytically and the results in terms of pressure traces or combustion metrics show that the design is very promising and robust to a good extent. Although the validation of this estimation design was validated using a 4-cylinder engine, the concept can be extended to “banks” of cylinders such as V6 or V8. A concern and future work would be the lack of Uniform Convergence in the adaptive estimator design although the main goal is yet achieved by proving convergence of the cylinder pressure state.

## APPENDIX NOMENCLATURE

$P_{max}$	Maximum pressure
$CA_{50}$	Crank angle location for 50% burn fraction
$IMEP$	Indicated mean effective pressure
$IVC$	Intake valve closing
$EVO$	Exhaust valve opening
$\gamma$	Polytropic coefficient
$V_{cyl}$	Cylinder Volume
$\theta$	Crank angle
$Q_g$	Apparent gross heat release
$A_p$	Piston bowl cross-sectional area
$p_{amb}$	Ambient pressure
$TDC$	Top dead center
$\tau_{ind}$	Indicated torque
$\tau_{mass}$	Reciprocating inertia torque
$\tau_{fric}$	Friction torque
$\tau_{load}$	Load torque
$J_{eq}$	Equivalent mass moments of inertia
$\omega$	Crank shaft speed
$SMO$	Sliding mode observer
$V_{eq}$	Equivalent control
$\mu$	Uncertainty parameter
$rem$	Remainder function.

## LA SALLE/YOSHIZAWA THEOREM

The La Salle/Yoshizawa theorem is similar to the well know theorem by La Salle for asymptotic stability of autonomous systems [23]. However, this theorem deals with non-autonomous systems. The theorem can be stated as follows:

For the non-autonomous system  $\dot{x} = f(t, x)$ , where  $f$  is piecewise continuous function in  $t$  and locally Lipschitz in  $x \in \mathbb{R}^n$ .

Assume  $\exists W(x) \geq 0$  and  $V(t, x)$  such that:

$$\underline{\alpha}(|x|) \leq V(t, x) \leq \bar{\alpha}(|x|), \quad \text{where } \underline{\alpha}, \bar{\alpha} \in K_{\infty}.$$

and

$$\frac{\partial V}{\partial t} + \frac{\partial V}{\partial x} f(t, x) \leq -W(x), \quad \forall t \in \mathbb{R}, \forall x \in \mathbb{R}^n.$$

Then:

- 1) Trajectories  $x(t)$  are bounded.
- 2)  $x = 0$  is uniformly stable (US) in the sense of Lyapunov.
- 3)  $\forall (t_0, x_0) \in \mathbb{R} \times \mathbb{R}^n \quad W(x(t)) \rightarrow 0$ .

## ACKNOWLEDGMENT

The author would like to thank the Center for Automotive Research, The Ohio State University for providing support to the work presented in this paper.

## REFERENCES

- [1] Robert Bosch GmbH, *Diesel-Engine Management Handbook*. Cambridge, MA, USA: Bentley, 2008.
- [2] R. Maringanti, S. Midlam-Mohler, M. Fang, F. Chiara, and M. Canova, "Set-point generation using kernel-based methods for closed-loop combustion control of a CIDI engine," in *Proc. Dyn. Syst. Control Conf.*, Oct. 2009, pp. 565–572.
- [3] M. Fang, S. Midlam-Mohler, R. Maringanti, F. Chiara, and M. Canova, "Optimal performance of cylinder-by-cylinder and fuel bank controllers for a CIDI engine," in *Proc. Dyn. Syst. Control Conf.*, 2009, pp. 573–580.
- [4] E. Corti, D. Moro, and L. Solieri, "Real-time evaluation of IMEP and ROHR-related parameters," SAE Tech. Paper 2007-24-0068, Sep. 2007.

- [5] Y. Shiao and J. J. Moskwa, "Cylinder pressure and combustion heat release estimation for SI engine diagnostics using nonlinear sliding observers," *IEEE Trans. Control Syst. Technol.*, vol. 3, no. 1, pp. 70–78, Mar. 1995.
- [6] G. Rizzoni, "Estimate of indicated torque from crankshaft speed fluctuations: A model for the dynamics of the IC engine," *IEEE Trans. Veh. Technol.*, vol. 38, no. 3, pp. 168–179, Aug. 1989.
- [7] Y.-Y. Wang, V. Krishnaswami, and G. Rizzoni, "Event-based estimation of indicated torque for IC engines using sliding-mode observers," *Control Eng. Pract.*, vol. 5, no. 8, pp. 1123–1129, 1997.
- [8] Y. Guezennec and P. Gyan, "A novel approach to real-time estimation of the individual cylinder combustion pressure for S.I. engine control," in *Proc. SAE Int. Congr. Expo.*, 1999, paper 1999-01-0209, doi: 10.4271/1999-01-0209.
- [9] D. Moro, N. Cavina, and F. Ponti, "In-cylinder pressure reconstruction based on instantaneous engine speed signal," *J. Eng. Gas Turbines Power*, vol. 124, no. 1, pp. 220–225, 2002.
- [10] D. Brand, C. Onder, and L. Guzzella, "Estimation of the instantaneous in-cylinder pressure for control purposes using crankshaft angular velocity," in *Proc. SAE World Congr.*, 2005, paper 2005-01-0228, doi: 10.4271/2005-01-0228.
- [11] Y. Shiao and J. Moskwa, "Misfire detection and cylinder pressure reconstruction for SI engines," in *Proc. SAE Int. Congr. Expo.*, Mar. 1994, paper 940144, doi: 10.4271/940144.
- [12] F. T. Connolly and G. Rizzoni, "Real time estimation of engine torque for the detection of engine misfires," *J. Dyn. Syst., Meas., Control*, vol. 116, no. 4, pp. 675–686, 1994.
- [13] D. Lee and G. Rizzoni, "Detection of partial misfire in IC engines using a measurement of crankshaft angular velocity," SAE Tech. Paper 951070, 1995.
- [14] A. Al-Durra, M. Canova, and S. Yurkovich, "A model-based methodology for on-line estimation of diesel engine cylinder pressure," *J. Dyn. Syst., Meas., Control*, vol. 133, no. 3, pp. 031005-1–031005-9, Mar. 2011, doi: 10.1115/1.4003370.
- [15] J. Heywood, *Internal Combustion Engine Fundamentals*. New York, NY, USA: McGraw-Hill, 1988.
- [16] F. Ponti, G. Serra, and C. Siviero, "A phenomenological combustion model for common rail multi-jet diesel engine," in *Proc. ASME ICE Fall Tech. Conf.*, 2004, pp. 437–446.
- [17] I. Haskara and L. Mianzo, "Real-time cylinder pressure and indicated torque estimation via second order sliding modes," in *Proc. Amer. Control Conf.*, 2001, pp. 3324–3328.
- [18] M. Canova, Y. Guezennec, and S. Yurkovich, "On the control of engine start/stop dynamics in a hybrid electric vehicle," *J. Dyn. Syst., Meas., Control*, vol. 131, no. 6, pp. 061005-1–061005-12, Nov. 2009.
- [19] H. Hamedović, F. Raichle, J. Breuninger, W. Fischer, W. Dieterle, and M. Klenk, "IMEP-estimation and in-cylinder pressure reconstruction for multicylinder SI-engine by combined processing of engine speed and one cylinder pressure," in *Proc. SAE World Congr.*, Apr. 2005, paper 2005-01-0053, doi: 10.4271/2005-01-0053.
- [20] A. Al-Durra, M. Canova, and S. Yurkovich, "Application of extended Kalman filter to on-line diesel engine cylinder pressure estimation," in *Proc. Dyn. Syst. Control Conf.*, Oct. 2009, pp. 541–548.
- [21] A. Al-Durra, L. Fiorentini, M. Canova, and S. Yurkovich, "A model-based estimator of engine cylinder pressure imbalance for combustion feedback control applications," in *Proc. Amer. Control Conf.*, Jun. 2011, no. 561, pp. 991–996.
- [22] A. Isidori, *Nonlinear Control Systems*. London, U.K.: Springer-Verlag, 1995.
- [23] H. Khalil, *Nonlinear Systems*. Upper Saddle River, NJ, USA: Prentice-Hall, 2002.

**AHMED AL-DURRA** (S'07–M'10–SM'14) received the B.S., M.S., and Ph.D. degrees in electrical and computer engineering from the Ohio State University, Columbus, OH, USA, in 2005, 2007, and 2010, respectively. For his M.Sc. degree, he investigated the application of several nonlinear control techniques on automotive traction PEM fuel cell systems. He conducted his Ph.D. research with the Center for Automotive Research, Ohio State University. His Ph.D. work was on the applications of modern estimation and control theories to automotive propulsion systems. He is working as an Assistant Professor with the Department of Electrical Engineering and the Downstream Research Coordinator of the PI Research Center with the Petroleum Institute, Abu Dhabi, United Arab Emirates. His research interests are application of estimation and control theory in power system stability and control, energy storage system, renewable energy, and process control. Dr. Al-durra is a member of ASME.